J. CHEM. SOC. FARADAY TRANS., 1990, 86(20), 3405–3411

Kinetics of Redox Dissolution of Soft-centre Particles

Andrew Mills* and David Worsley
Department of Chemistry, University College of Swansea, Singleton Park, Swansea SA2 8PP, Wales

A model is developed which describes the kinetics of redox dissolution of a powder comprising soft-centre particles, *i.e.* particles with a comparatively inert, outer layer and a more reactive, inner core. The model is then used to interpret the non-simple cubic rate law kinetics exhibited in the oxidative dissolution of partially dehydrated samples of ruthenium dioxide hydrate by bromate ions under acidic conditions.

Redox dissolution, *i.e.* the dissolution of particulate matter by either a reducing agent or an oxidising agent, has received increased attention over recent years because of its relevance to the decontamination of nuclear plants and oxide scale removal in industry.[1] Although much of the research is directed towards improving the associated technology, more fundamental studies into the kinetics of dissolution are a growing area of interest. It has emerged from many of these studies that the kinetics of particle dissolution can be modelled very well by assuming that the particles are spherical and monodispersed, and that at any time during the dissolution process the rate is proportional to the total instantaneous surface area due to the particles.[1] Given these assumptions, the well known[2] simple cubic rate law can be derived, *i.e.*

$$1 - (m_t/m_0)^{1/3} = kt/(r_0\rho) \quad (1)$$

where m_0 and m_t are the total masses of undissolved particles at $t = 0$ and $t = t$, respectively, r_0 is the initial radius of the particles at $t = 0$ and ρ is the density of the particulate material.

In a recent paper[3] we developed a model which describes how the kinetics of dissolution deviate from the simple cubic rate law if the particles are polydispersed, rather than monodispersed, and the variation in particle size fits a log-normal distribution. This model was used to analyse kinetic data reported for the dissolution of a polydispersed powder suspension and determine the extent of the distribution in particle size in this powder. Support for the model was provided by the good match obtained between the experimental and model-predicted theoretical plots of relative volume *vs.* particle diameter for the powder dispersion.

Although deviations from a simple cubic rate law may be caused by an initial distribution in particle size, they may also be caused by factors which change during the dissolution process, such as the physical or chemical nature of the material. One likely example of a cause for deviation from a simple cubic rate law dependence would be if the spherical particles were not homogeneous in composition but comprised an outer layer which is relatively inert towards dissolution and an inner, more reactive core; such particles could be termed 'soft-centred'. The two different dissolution reactivities exhibited by the different parts of a soft-centre particle could be due to a change in the physical nature of the material (such as degree of crystallinity) or a change in the chemical nature of the material (such as a metal oxide outer layer/metal core combination). In this paper we describe a model for the kinetics of dissolution of a monodispersion of soft-centre particles and its subsequent use in characterising a real system which involves the oxidative dissolution of particles of partially dehydrated samples of ruthenium dioxide hydrate by bromate ions under acidic conditions.

Experimental

Materials

The ruthenium dioxide hydrate sample used had a water content of 23.5% and was obtained from Johnson Matthey (batch no. 061 301B). The sodium bromate was obtained from BDH as a general-purpose reagent and used as received. All other chemicals were obtained from BDH in the highest purity available. The water used to make up solutions was doubly distilled and deionised. All reactions were carried out in 0.5 mol dm^{-3} H_2SO_4 at 30 °C. The ruthenium tetraoxide used in this work was prepared from ruthenium dioxide hydrate powder using a procedure which is described elsewhere,[4] with periodate as the oxidising agent.

Methods

The kinetics of oxidative dissolution of different samples of ruthenium dioxide hydrate by bromate ions were monitored spectrophotometrically *via* the appearance of RuO_4. For each kinetic 'run' two absorbance *vs.* time profiles were recorded under identical reaction conditions; the first at 309 nm where the absorbance changes are due to RuO_4 generation and powder dissolution, and the second at 700 nm where the absorbance changes are due to powder dissolution alone. For each 'run' the second of these absorbance *vs.* t profile was subtracted from the first and the resultant absorbance *vs.* time profiles taken as being solely due to the variation in $[RuO_4]$ *vs.* t. A more detailed description of the methods used is given elsewhere.[5]

The kinetic runs were carried out in a 1 cm fluorescence cell and the powder suspension was stirred continuously using a Teflon-covered magnetic flea rotating at a fixed rate. In a typical run 100 mm^3 of 0.1 mol dm^{-3} $NaBrO_3$ in 0.5 mol dm^{-3} H_2SO_4 was injected into a 2.5 cm^3 of 0.5 mol dm^{-3} H_2SO_4 containing the sample of ruthenium dioxide hydrate under study (typically 60 mg dm^{-3}). After subtracting the contribution of the decrease in absorbance due to the powder as the dissolution proceeds, the resultant plot of normalised absorbance due to RuO_4 (where the absorbance at $t = \infty$ due to RuO_4 was taken as 1) *vs.* time was then analysed according to the soft-centre model using a microcomputer and the best-fit values of f, g and h obtained.

Particle-size analysis of the powder dispersions used was carried out by a dynamic light scattering technique using a Malvern instruments model S3.01.

Soft-centre Model

Consider the general dissolution reaction

$$aX + bY \rightarrow cZ + dQ \quad (2)$$

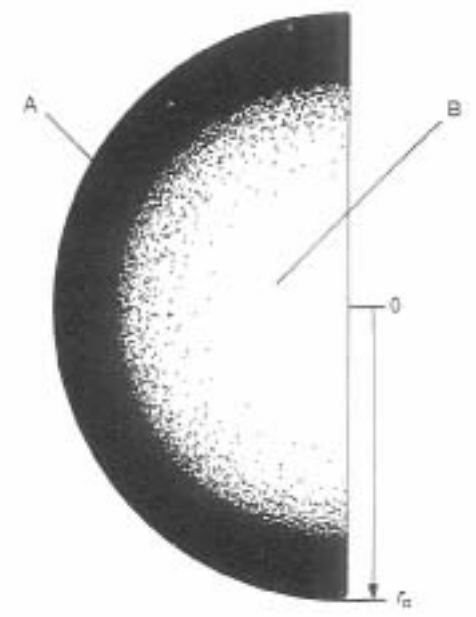

Fig. 1. Schematic illustration of a soft-centre particle showing the graduation from the more passive, outer layer A (dark) to the reactive inner layer material B (light).

where X is a powder comprising monodispersed, soft-centre particles of initial radius, r_0, dispersed in solution and which dissolve to form Z in a redox reaction involving Y which, in turn, forms Q. The terms *a*, *b*, *c* and *d* are the appropriate reaction stoichiometries. In this scheme Y, Z and Q are assumed to be homogeneous species, the presence of which does not limit the rate of dissolution. In addition, it is assumed that the rate-limiting step in the dissolution process involves reaction at the particle's surface and, therefore, at any time, *t*, the rate is proportional to the instantaneous surface area, $A(\text{total})_t$, *i.e.*

$$\mathrm{d}m/\mathrm{d}t = -kA(\text{total})_t \qquad (3)$$

where *m* is the mass of undissolved particles of X (in g) and *k* is the rate constant (in g m^{-2} s^{-1}), which is dependent upon the nature of X and the surface concentration of Z. Integration of eqn (3) yields the simple cubic rate law, eqn (1).

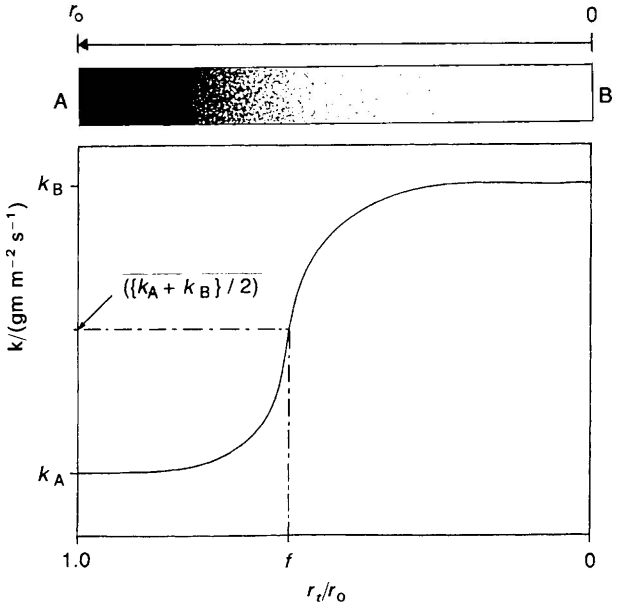

Fig. 2. Schematic illustration of the expected variation in *k* as a function of r_t/r_0 for a soft-centre particle.

The simple cubic rate law assumes that the chemical and physical nature of X is invariant throughout the particle and, as a result, *k* can be considered to be constant as the particle dissolves. However, this need not be the case, and one plausible alternative scenario would be that each of the particles comprises a fairly unreactive outer layer (material A) and a more reactive inner core (material B), as illustrated in fig. 1. Given this model, it seems reasonable to assume that the rate constant, *k*, in eqn (3) would vary as the degree of dissolution [a measure of which is the term $(1 - r_t/r_0)$] increased in the manner illustrated in fig. 2. An expression which describes the variation of *k* as a function of r_t/r_0, similar to that illustrated in fig. 2, is as follows:

$$(k - k_A)/(k_B - k) = \exp\{[(r_0 - r_t) - fr_0]g/r_0\} \qquad (4)$$

where *f* and *g* are two constants which determine the relative thicknesses of the two layers and the sharpness of the transition between materials A and B, respectively. If we define a third parameter, *h*, as the ratio of the rate constant for dissolution of pure A to that of pure B, *i.e.*

$$h = k_A/k_B \qquad (5)$$

then, eqn (4) can be rewritten as

$$k = k_B[\exp(\theta) + h]/[1 + \exp(\theta)] \qquad (6)$$

where $\theta = [(r_0 - r_t) - fr_0]g/r_0$.

Effect on *k* of the Parameters *f*, *g* and *h*

As indicated in eqn (6), in this soft-centre model the observed rate constant depends upon the values selected for *f*, *g* and *h* and it is appropriate to examine the effect that different values of each of these parameters has on *k* before developing an expression which predicts the dissolution kinetics under these conditions.

Technically, the constant *f* is the ratio of the radius of the partially dissolved particle at time *t*, when $k = (k_A + k_B)/2$, to its initial radius at $t = 0$, *i.e.*

$$f = r_t/r_0 \qquad (7)$$

and its value may lie anywhere in the range $0 \leqslant f \leqslant 1$. In effect, however, *f* provides a guide to the thickness of the passive layer since the larger the value of *f* the greater the fraction of the particle's mass is composed of the more inert, outer material A. Fig. 3(*a*) illustrates the variation in k/k_B *vs.* r_t/r_0 calculated using eqn (6), where *f* is varied from 0 to 1 and *g* and *h* are fixed at intermediate values of 10 and 0.1, respectively.

The value of the constant, *g*, which must be $\geqslant 0$, describes the nature of the transition of *k* from its initial low value to its final higher value as dissolution of the particle proceeds and, as such, reflects the nature of the boundary between the outer and inner types of material. For example, if *g* is large the boundary will be sharp and if *g* is small the boundary will be diffuse. The effect of *g* on *k* is illustrated in fig. 3(*b*) with the variation in k/k_B *vs.* r_t/r_0 calculated using eqn (6), where *g* is varied from 0 to 100 and *f* and *h* are both fixed at a typical intermediate value of 0.1.

The constant *h*, which is defined in eqn (5) and must have a value $\leqslant 1$ for a soft-centred particle, provides a measure of the difference in dissolution reactivities of the two pure materials, A and B, which make up the particle. The effect of different values of *h* on *k* as the dissolution proceeds is illustrated in fig. 3(*c*) with the variation in k/k_B *vs.* r_t/r_0 calculated using eqn (6), where *h* is varied from 1 to 0.001 and *f* and *h* are fixed at 10 and 0.1, respectively.

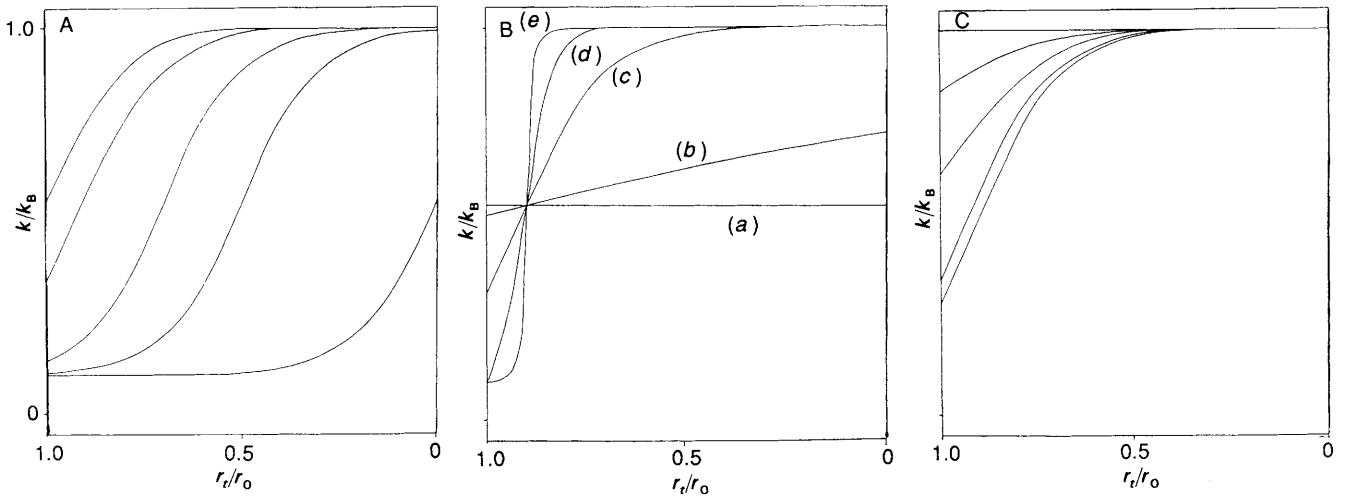

Fig. 3. Theoretical plots of k/k_B *vs.* r_t/r_0 calculated using eqn (6) of the soft-centre model and the following values for f, g and h: (A) $g = 10$, $h = 0.1$ and, from left to right, $f = 0$, 0.1, 0.3, 0.5 and 1, respectively; (B) $f = h = 0.1$ and, $g =$ (*a*) 0, (*b*) 1, (*c*) 30, (*d*) 50 and (*e*) 100, respectively; (C) $g = 10$, $f = 0.1$ and, from top to bottom, $h = 1$, 0.8, 0.5, 0.1 and 0.001, respectively.

The dissolution kinetics for the particles under consideration (see fig. 1) will obey the simple cubic rate law provided k is constant as dissolution of a particle proceeds, *i.e.* as r_t/r_0 varies from 1 to 0. A brief examination of eqn (6) and fig. 3 indicates that this condition will be fulfilled for the following cases: (i) $f = 0$ or 1, $g = \infty$, $h =$ any value; (ii) $f =$ any value, $g = 0$, $h =$ any value; (iii) $f =$ any value, $g =$ any value, $h = 1$.

Predicted Dissolution Kinetics for Soft-centred Particles

Substitution for k, as defined in eqn (6), into eqn (3) and subsequent integration yields the following expression:

$$\tau = (1 - r_t/r_0)(1 + 1/h) - (1/hg)\ln\{[h + \exp(\theta)]/[h + \exp(-fg)]\} + (1/g)\ln\{[1 + h\exp(-\theta)]/[1 + h\exp(fg)]\} \quad (8)$$

where τ is a dimensionless parameter which is directly related to the time of dissolution t, *via* the expression:

$$\tau = k_B t/(\rho r_0). \quad (9)$$

In practice, it is often difficult to monitor, as dissolution proceeds, the variation of the ratio r_t/r_0 as function of time and, instead, the ratio of the total mass of undissolved particles at time t to that at $t = 0$, *i.e.* $m_t(\text{total})/m_{t=0}(\text{total})$ is often monitored. The two ratios are related by the expression

$$r_t/r_0 = [m_t(\text{total})/m_{t=0}(\text{total})]^{1/3} \quad (10)$$

assuming that the densities of the two materials A and B are the same. Alternatively, in some cases it is possible to measure the concentration of Z as a function of time, *i.e.* $[Z]_t$, as the dissolution proceeds (*via* UV–VIS absorption spectroscopy for example) and this allows the parameter r_t/r_0 to be calculated at time t, since they are related *via* the expression

$$r_t/r_0 = \{1 - ([Z]_t/[Z]_\infty)\}^{1/3} \quad (11)$$

where $[Z]_\infty$ is the concentration of Z when the dissolution reaction has gone to completion.

It is useful to compare the kinetics of dissolution predicted using the conventional simple cubic rate law, which assumes the particles to be homogeneous in composition, and the modified cubic rate law, as defined by eqn (8), which assumes the particles to be soft-centred. Using the simple cubic rate law the kinetics of dissolution of powder particles comprising only material B would be described by the following expression:

$$\tau = 1 - \{1 - ([Z]_t/[Z]_\infty)\}^{1/3} \quad (12)$$

where τ is defined by eqn (9) and can have any value in the range $0 \leqslant \tau \leqslant 1$. Eqn (12) and (8) can be used to predict the variation of $[Z]_t/[Z]_\infty$ *vs.* τ for the dissolution of homogeneous and heterogeneous soft-centre particles, respectively, and the results are illustrated in fig. 4A, with curves (*a*) and (*b*) corresponding to the homogeneous and soft-centre cases, respectively. From the two curves illustrated in fig. 4A it is clear that the kinetics of dissolution of soft-centre particles compared with that of homogeneous particles can be very different, even if the outer layer of material A in the latter particles is thin, as is the case in the example illustrated in fig. 4A, curve (*b*), where f was set at 0.1.

The difference between the two types of dissolution kinetics is even more striking if the data are plotted in the conventional simple cubic rate law form, *i.e.* $\{1 - ([Z]_t/[Z]_\infty)\}^{1/3}$ *vs.* τ, as illustrated in fig. 4B. Note that in the case of the soft-centre dissolution kinetics, the simple cubic rate law plot of the data [curve (*b*), fig. 4B], appears a clear combination of two straight lines with gradients w_A (small) and w_B (large), respectively. Not surprisingly, the ratio w_A/w_B (=0.1/1) provides an excellent approximation of the parameter h (=0.1). In addition the y coordinate of extrapolated point at which these two lines intercept [indicated on fig. 4B by an arrow and =0.89] provides a reasonable approximation of the term $(1 - f)$ and, therefore, f itself (=0.1). As a result, when the kinetics of dissolution for a real system, show deviations of the nature illustrated in fig. 4. then a simple cubic rate law plot of the data, such as illustrated in fig. 4B, will, in many cases, provide a good estimate of the first two of the three parameters, h, f and g, and, as we shall see in the next section, this can facilitate the accurate determination of all three parameters.

Note at this point that the kinetics of dissolution exhibited by a soft-centre model are very different from those exhibited by a model in which there is a range of initial particle sizes. Work carried out by ourselves[3] and others[2] into modelling the kinetics of dissolution of a polydispersion with a log-normal or Gaussian distribution in particle size shows that the rate of dissolution will be initially high and fall below

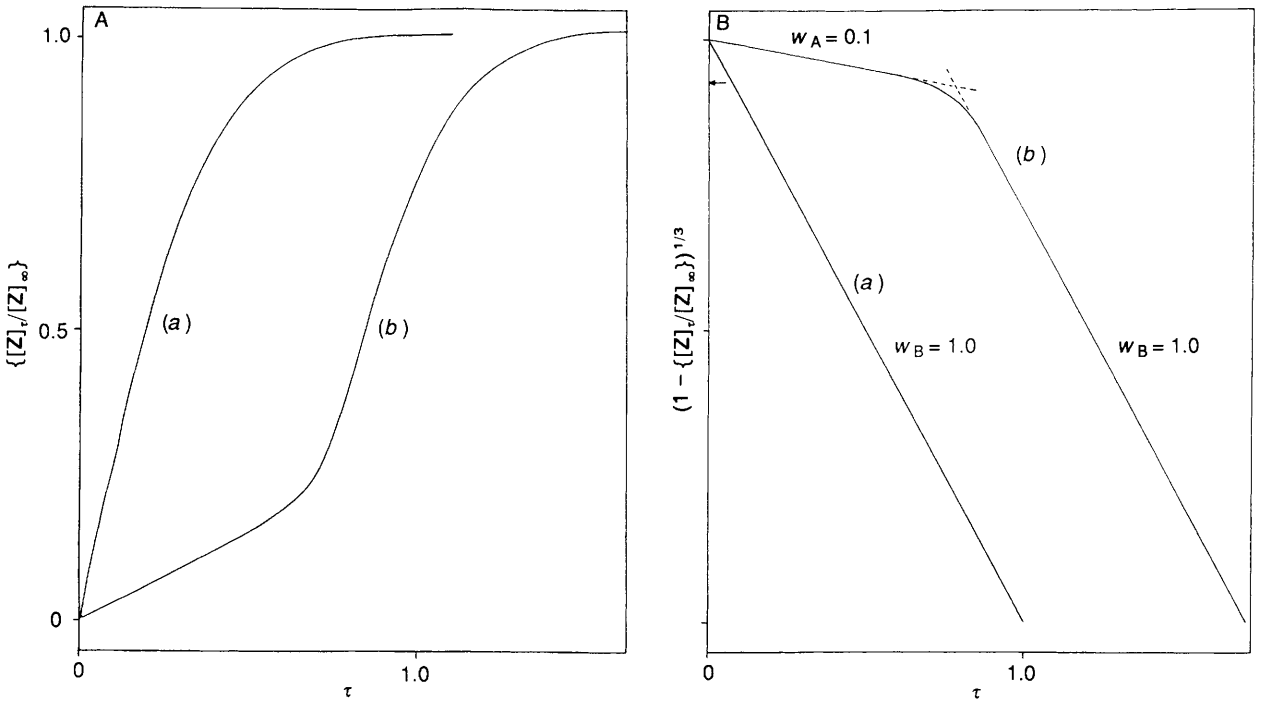

Fig. 4. Plots of dissolution kinetic data predicted using (*a*) the simple cubic rate law [*i.e.* eqn (12)] and (*b*) the soft-centre model [*i.e.* eqn (8), with $f = h = 0.1$ and $g = 100$] in the form of (A) $[Z]_t/[Z]_\infty$ *vs.* τ and (B) $\{1 - ([Z]_t/[Z]_\infty)\}^{1/3}$ *vs.* τ (conventional cubic rate law plot).

that predicted from a simple cubic law model as the reaction proceeds. A simple cubic rate plot (*i.e.* $\{1 - ([Z]_t/[Z]_\infty)\}^{1/3}$ *vs.* τ) of the predicted dissolution data for powder suspension with a log-normal distribution of particle sizes gives an initial straight line which shows an increasing positive deviation with time. Interestingly, although these latter kinetics are opposite to those predicted by the soft-centre model, they would be similar to those predicted by a hard-centre (soft shell) model.

Applying the Soft-centre Particle Model

In an experimental system in which the dissolution kinetics obey the soft centre model, knowledge of h, f and g is needed before the observed kinetics can be fully modelled, *via* eqn (8), and the important characteristic kinetic parameter, $k_B/(\rho r_0)$, extracted. In practice this can be achieved by plotting the real data in the form $([Z]_t/[Z]_\infty)$ *vs.* ln t and comparing the shape of the curve obtained with a series of theoretical curves plotted in the form $([Z]_\tau/[Z]_\infty)$ *vs.* ln τ and generated *via* eqn (8) using a range of different values of f, g and h. No two theoretical curves with different values of f, g and h are identical in shape and, thus, the theoretical curve which gives the best fit with the real data will, ideally, have the same values of f, g and h as the real system. In practice the experimental error associated with the data will determine the errors in the values of f, g and h.

In fig. 5(*a*)–(*c*) plots of $([Z]_\tau/[Z]_\infty)$ *vs.* ln τ are illustrated where, respectively, the parameters, f, g and h have been systematically varied in a fashion similar to that used to illustrate the effect of these parameters on k [see fig. 3(*a*)–(*c*)]. By comparing the shape of the plot of experimental kinetic dissolution data in the form of $([Z]_t/[Z]_\infty)$ *vs.* ln t with families of theoretical curves such as those illustrated in fig. 5(*a*)–(*c*), it is possible to obtain quite good estimates of f, g and h. However, more accurate values of f, g and h can be obtained through the use of a computer program designed to find the values of these parameters which generate, *via* eqn (8) of the soft-centre model, a theoretical $([Z]_\tau/[Z]_\infty)$ *vs.* ln τ curve which has the closest fit in shape to the experimentally determined kinetic dissolution data plotted in the form $([Z]_t/[Z]_\infty)$ *vs.* ln t. In the previous section we noted that values of f and h can be readily estimated in some cases from a plot of the experimental kinetic dissolution data in the form of $\{1 - ([Z]_t/[Z]_\infty)\}^{1/3}$ *vs.* t [see fig. 4B]. This approach, coupled with the simple comparison procedure described above, provides good initial estimates of the values of all three parameters which characterise the best-fit soft-centre theoretical curve and this, in turn, cuts down the computing time required to identify the 'best-fit' values of f, g and h.

Once the parameters f, g and h have been determined for an experimental $([Z]_t/[Z]_\infty)$ *vs.* ln t curve, it is a relatively simple task to determine the important parameter, $k_B/(\rho r_0)$, which characterises the kinetics of dissolution of material B and, *via* eqn (5), material A. This step requires the determination of the numerical difference between ln t and ln τ for any two points on the appropriate experimental and theoretical plots with the same value of $([Z]_t/[Z]_\infty)$ and $([Z]_\tau/[Z]_\infty)$, respectively. Under these conditions, the measured difference, *i.e.* $|\ln t - \ln \tau|$, will be equal to $\ln[k_B/(\rho r_0)]$ [see eqn (9)] as illustrated in fig. 6. Access to the parameter $k_B/(\rho r_0)$ allows the kinetics of dissolution to be further characterised by studying $k_B/(\rho r_0)$ as a function of [X], [Y] and temperature.

Dissolution of Partially Dehydrated Ruthenium Dioxide Hydrate

In a previous paper[5] we described the results of a kinetic study involving the oxidative dissolution of fully hydrated ruthenium dioxide hydrate powder, $RuO_2 \cdot xH_2O$, by bromate ions (BrO_3^-) under acidic conditions (0.5 mol dm^{-3} H_2SO_4). In this work we found that a highly hydrated sample of $RuO_2 \cdot xH_2O$ (H_2O *ca.* 24–26%) underwent oxidative dissolution to form ruthenium tetraoxide according to the stoichiometry

$$3RuO_2 \cdot xH_2O + 2BrO_3^- \rightarrow 3RuO_4 + 2Br^- + 3xH_2O. \quad (13)$$

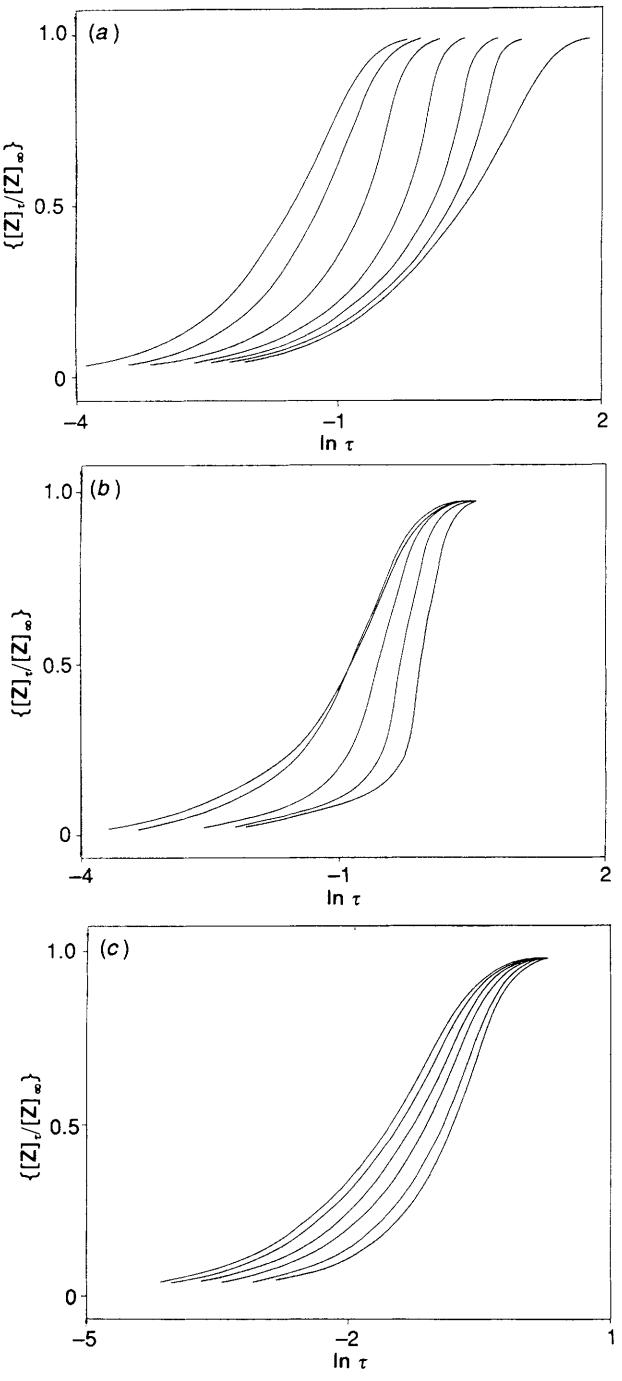

Fig. 5. Plots of $([Z]_\tau/[Z]_\infty)$ *vs.* ln τ, calculated using eqn (8) for the following conditions: (*a*) $h = 0.1$, $g = 10$ and, from left to right, $f = 0$, 0.1, 0.2, 0.3, 0.4, 0.5 and 1.0, respectively; (*b*) $f = h = 0.1$ and, from left to right, $g = 5$, 10, 30, 50 and 100, respectively; (*c*) $f = 0.1$, $g = 10$ and, from left to right, $h = 1.0$, 0.8, 0.5, 0.3, 0.1 and 0.01, respectively.

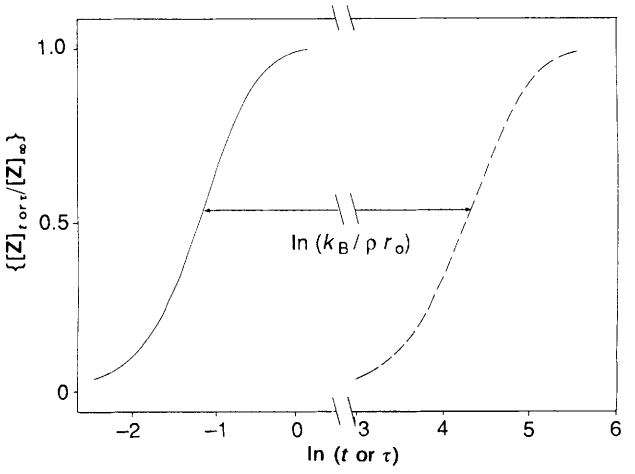

Fig. 6. Schematic illustration of the method of calculating $\ln[k_B/(\rho r_0)]$. Both the experimental dissolution kinetic data (– – –) and the best-fit soft-centre theoretical data (——) are plotted in the form $([Z]_{t \text{ or } \tau}/[Z]_\infty)$ *vs.* ln(t or τ). As indicated in the diagram, the difference between ln τ and ln t for any two points with the same value of $([Z]_{t \text{ or } \tau}/[Z]_\infty)$ which lie on these two curves, respectively, is $\ln[k_B/(\rho r_0)]$.

The kinetics of reaction (13) were found to obey the simple cubic rate law, eqn (1), and the constant $k/(\rho r_0)$ was studied as a function of $[BrO_3^-]$, $[RuO_2 \cdot xH_2O]$ and temperature. In previous papers[6,7] we noted that when $RuO_2 \cdot xH_2O$ ($H_2O \geqslant 24\%$) is heat-treated prior to its use, it exhibits a resistance towards oxidative dissolution which increases with increasing annealing temperature. Indeed, by using an annealing temperature of only 150 °C (5 h in air) the partially dehydrated ruthenium dioxide hydrate powder, referred to as 'thermally activated ruthenium dioxide hydrate' or $RuO_2 \cdot yH_2O$*, is made largely corrosion-resistant, as judged by the experimental conditions employed to test this property, even though its water content remains high ($H_2O \approx$ 10%). (Despite this there does seem to be a strong link between H_2O content and corrosibility with samples of hydrated ruthenium dioxide).[7]

The fully hydrated and thermally activated forms of ruthenium dioxide hydrate represent two extremes in behaviour with regard to oxidative dissolution. Samples of ruthenium dioxide hydrate with intermediate water contents (*i.e.* $11 \leqslant H_2O(\%) \leqslant 24$) may be synthesised by the aerobic alkaline hydrolysis of commercial ruthenium trichloride and subsequent drying at above ambient temperature (but well below 150 °C) or, in some cases, purchased (the H_2O content of different batches of this material can vary by as much as 15% from the same supplier!).

In this work we studied the kinetics of oxidative dissolution of these intermediate samples of ruthenium dioxide hydrate and found that they do not fit the simple cubic rate law, but instead show an induction period which increases with increasing annealing temperature and corresponding decreasing H_2O content. This effect is illustrated in fig. 7, which is a plot of the observed variation in normalised absorbance due to RuO_4 production *via* reaction (13) *vs.* time after BrO_3^- addition for samples of ruthenium dioxide hydrate with H_2O contents of (*a*) 23.5, (*b*) 22 and (*c*) 19.5%, respectively. The variation in H_2O content was achieved by annealing the sample used in run (*a*) of fig. 7 at 50 °C [curve (*b*)] and 70 °C [curve (*c*)] for 1 h, respectively. Further experiments with initial background concentrations of RuO_4 up to five times that generated *via* reaction (13) showed that kinetics of dissolution were independent of the RuO_4 concentration, *i.e.* the induction period was not due to an autocatalytic reaction centring on the generation of RuO_4.

Particle-size analysis of the powder dispersions used showed that they had an average particle size of 6.1 μm and that the variation in size fitted a log-normal distribution with a narrow distribution width ($\gamma = 0.23$), *i.e.* with an error of ±1.4 μm. A model of the kinetics of dissolution of a powder dispersion with the same, narrow distribution revealed that a simple cubic rate plot of the data would only deviate significantly (*i.e.* > 1%), and then in a positive manner, after 91% of the powder had dissolved. This finding shows that for such a narrow dispersion the effect of varying particle size on the kinetics of dissolution is largely negligible and that the dispersion can be considered to be a monodisperse.

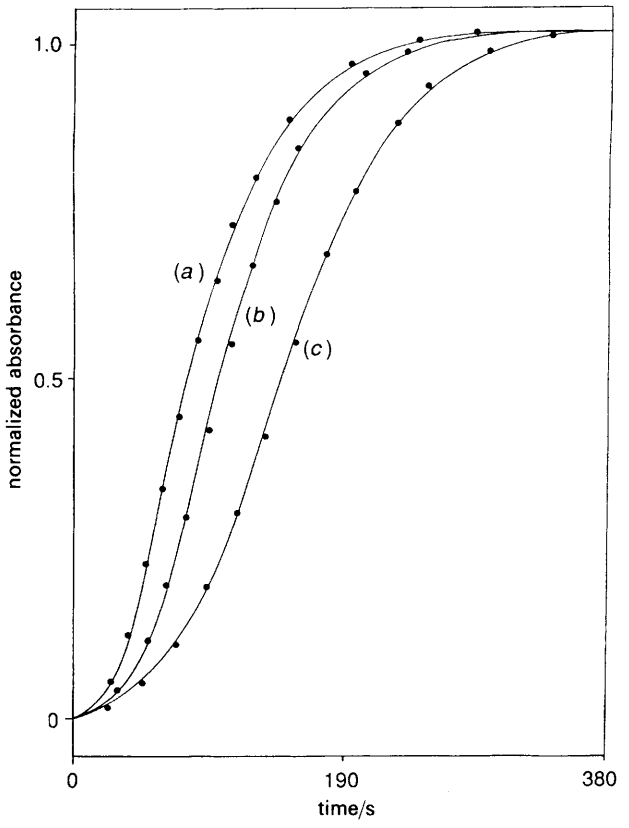

Fig. 7. Plot of normalised absorbance *vs.* time for the observed kinetics of dissolution of a sample of $RuO_2 \cdot xH_2O$ (Johnson Matthey, batch no. 061301B) which was annealed for 1 h in air prior to use and at the following temperatures (*a*) ambient, (*b*) 50 °C and (*c*) 70 °C. All other experimental conditions as described in the Experimental section.

The solid lines for curves (*a*)–(*c*) in fig. 7 are the optimised curves of best fit generated using eqn (8) of the soft-centre model. For each of these powders in table 1 the following information is given: the parameters *f*, *g* and *h* which define the optimised (solid line) theoretical plot, the value of $k_B/(\rho r_0)$, the measured surface areas and the H_2O content. From the results in table 1 it would appear that heat treatment of the powder increases the thickness of the comparatively inert, outer layer (*i.e.* *f* increases) and the boundary between the two layers becomes more diffuse (*g* decreases), although the rate constants for the two pure materials A (outer) and B (core) remain independent of temperature (*h* is constant).

Table 1. Ruthenium dioxide hydrate powder dissolution characteristics

sample[a] annealing temp./°C	optimised[b] values of *f*	*g*	*h*	$[k_B/(\rho r_0)]$ /s^{-1}	surface area[c] /$m^2\ g^{-1}$	H_2O (%)[d]
ambient	0.028	82	0.0028	0.0048	98	23.5
50	0.037	64	0.0028	0.0043	93	22
70	0.064	33	0.0028	0.0037	88	19.5

[a] Original ruthenium dioxide hydrate sample supplied by Johnson Matthey (batch no. 061301B). [b] Optimised with respect to *f*, *g* and *h* to give the best fit in shape between experimental and theoretical plots of $([Z]_t/[Z]_\infty)$ *vs.* ln *t* and $([Z]_t/[Z]_\infty)$ *vs.* ln τ, respectively. The error associated with each of the values of *f*, *g* and h is *ca.* 7%. [c] Measured by single-point B.E.T. with samples degassed for 48 h at ambient temperature under a continuous stream of nitrogen. [d] Measured using TG.

The soft-centre model appears appropriate for describing the kinetics of dissolution illustrated in fig. 7 of the intermediate samples of ruthenium dioxide hydrate, given the not too unrealistic assumption that the particles of each powder sample [*i.e.* (*a*)–(*c*) in fig. 7] comprise a fairly inert outer layer, composed of material (material A similar, if not identical, to $RuO_2 \cdot yH_2O^*$, and a much more reactive inner core (material B), composed of fully hydrated ruthenium dioxide hydrate, *i.e.* $RuO_2 \cdot xH_2O$. Heating sample (*a*) at 50 and 70 °C to produce samples (*b*) and (*c*), respectively, would be expected to increase the thickness of the $RuO_2 \cdot yH_2O^*$ outer layer and decrease correspondingly the size of the $RuO_2 \cdot xH_2O$ core. This rationale is consistent with the calculated increase in *f* (see table 1) as the annealing temperature is increased. If, as we suggest, heat treatment simply converts some of the core $RuO_2 \cdot xH_2O$ to $RuO_2 \cdot yH_2O^*$ at the boundary, it seems consistent that the value of $h\ (=k_A/k_B)$ is independent of the heat treatment temperature and not surprising that the boundary between the two materials becomes less sharp as the annealing temperature is increased (see table 1).

When the soft-centre model is used to analyse the kinetics of dissolution illustrated in fig. 7 it appears that the parameter $k_B/(\rho r_0)$ decreases with increasing annealing temperature. At first this may appear to be inconsistent with the previous suggestion that k_A and k_B (and, therefore, *h*) are independent of annealing temperature since the variation of $k_B/(\rho r_0)$ with annealing temperature may be due to a decrease in k_B. It is possible that k_A and k_B decrease to the same extent with increasing annealing temperature and, thus, *h* is invariant. However, an alternative, and possibly more plausible explanation would be that k_B is independent of temperature, as initially assumed, and that the variation in $k_B/(\rho r_0)$ with *T* is due to a variation in the term, ρr_0. Interestingly, the surface area per g of a collection of monodispersed spherical particles is proportional to $(\rho r_0)^{-1}$. Thus, if the variation of $k_B/(\rho r_0)$ with annealing temperature is due to a temperature dependence exhibited by the denominator term then a parallel decrease in surface area would also be expected. The results given in table 1 appear to provide qualitative support for this suggestion, although this should be tempered with the recognition that the surface area data have an error of ±5% associated with them.

Conclusion

The soft-centre model of the redox dissolution of a powder dispersion comprising heterogeneous, spherical particles can be used to interpret the observed kinetics of oxidative dissolution of partially dehydrated samples of ruthenium dioxide hydrate by an excess of bromate ions. Interestingly, by considering values of $h > 1$, instead of < 1, the working equation of the soft-centre model, eqn (8), can be used to predict the dissolution kinetics of a hard-centre particle (*i.e.* a particle composed of a soft, or reactive, outer shell with a more inert core). The soft-centre model may have wide spread application and work is in progress to discover more systems where its application appears appropriate.

We thank the S.E.R.C. for supporting this work.

References

1 M. G. Segal and R. M. Sellers, *Adv. Inorg. Bioinorg. Mechn.*, 1984, **3**, 97, and references therein.
2 M. G. Segal and R. M. Sellers, *J. Chem. Soc., Faraday Trans. 1*, 1982, **78**, 1149.
3 A. Mills, H. L. Davies and M. Garley, *J. Chem. Soc., Faraday Trans.*, 1990, **86**, 2163.

4 A. Mills and N. McMurray, *J. Chem. Soc., Faraday Trans. 1*, 1988, **84**, 379.
5 A Mills and H. L. Davies, *J. Chem. Soc., Faraday Trans.*, 1990, **86**, 955.
6 A. Mills, S. Giddings and I. Patel, *J. Chem. Soc., Faraday Trans. 1*, 1987, **83**, 2317.
7 A. Mills and S. Giddings, *J. Chem. Soc., Faraday Trans. 1*, 1987, **83**, 2331.

Paper 0/01302A; *Received 26th March*, 1990